Smart Structures and Systems, *Vol. 20, No. 1 (2017) 11-22*
DOI: https://doi.org/10.12989/sss.2017.20.1.011

Temperature effect analysis of a long-span cable-stayed bridge based on extreme strain estimation

Xia Yang[a], Jing Zhang* and Wei-Xin Ren[b]

School of Civil Engineering, Hefei University of Technology,
193 Tunxi Road, Hefei City, Anhui Province, Republic of China

(Received December 28, 2016, Revised April 20, 2017, Accepted April 25, 2017)

Abstract. The long-term effect of ambient temperature on bridge strain is an important and challenging problem. To investigate this issue, one year data of strain and ambient temperature of a long-span cable-stayed bridge is studied in this paper. The measured strain-time history is decomposed into two parts to obtain the strains due to vehicle load and temperature alone. A linear regression model between the temperature and the strain due to temperature is established. It is shown that for every 1℃ increase in temperature, the stress is increased by 0.148 MPa. Furthermore, the extreme value distributions of the strains due to vehicle load, temperature and the combination effect of them during the remaining service period are estimated by the average conditional exceedance rate approach. This approach avoids the problem of declustering of data to ensure independence. The estimated results demonstrate that the 95% quantile of the extreme strain distribution due to temperature is up to 1.488×10^{-4} which is 2.38 times larger than that due to vehicle load. The study also indicates that the estimated extreme strain can reflect the long-term effect of temperature on bridge strain state, which has reference significance for the reliability estimation and safety assessment.

Keywords: average conditional exceedance rate method; bridge health monitoring; extreme strain; Monte Carlo; temperature effect

1. Introduction

Structural health monitoring has become increasingly important to assure structural safety and reliability. As one of the monitoring items, strain reflects the stress state of in-service bridges directly, providing an important basis for bridge safety assessment. To acquire more strain information, a large number of strain sensors are deployed in the structural health monitoring systems. For example, 140 strain gauges were installed on the Tsing Ma Bridge in Hong Kong (Wong 2004), and 80 strain sensors were adopted on the Runyang Yangtze River Bridge in China (Li *et al.* 2009). In addition, 80 fiber optic strain gauges were added into the upgrading and modifying project of Jiangyin Yangtze River Highway Bridge Structural Health Monitoring System (Han 2006).

Recently, attentions have been paid to the temperature effect on bridge strain especially for those statically indeterminate bridges since the impact is significant (Catbas 2008, Duan *et al.* 2010). Severe cracking caused by temperature effect are observed, such as the Jagst Bridge in Germany and several viaducts in United States (Branco and Mendes 1993). The environmental temperature effect on strain state of bridges should be taken into account to achieve reliable results of load analysis, state evaluation and so on. A large volume of research work has been conducted to investigate the impact of temperature gradient on stress condition of bridges (Krkoška and Moravčík 2015, Saetta *et al.* 1995). In addition, some researchers have separated the temperature effect from the measured strain data. Wu et al. (2014) decomposed the measured strain-time history of Tsing Ma Bridge in Hong Kong into two parts which are due to temperature and vehicle load, and results showed that strain due to temperature variation in 24 hours was greater than that due to the heaviest vehicle on the bridge in the same day. Same conclusion has been drawn based on the strain data acquired from the structural health monitoring system installed on the Baling River Bridge in China (Li *et al.* 2014).

In this paper, the extreme value (EV) of the strain due to temperature is estimated because the value is closely related to the safety of in-service bridges. For those conventional EV estimation methods, such as peaks-over-threshold (POT) method and block maxima method, sampled data required need to be statistically independent and identically distributed (Obrien *et al*. 2010, Gindy and Nassif 2006, James 2003). However, temperature variation is a continuous process with strong regularity. An obvious correlation is found between the sampled data of strain due to temperature. Therefore, the conventional methods are not suitable anymore. According to the conditional probability theory, the average conditional exceedance rate (ACER) approach is proposed (Karpa and Naess 2013). It has been

*Corresponding author, Associate Professor
E-mail: zhangj@hfut.edu.cn
[a] Ph.D. Student
E-mail: yangx@mail.hfut.edu.cn
[b] Professor
E-mail: renwx@hfut.edu.cn

ISSN: 1738-1584 (Print), 1738-1991 (Online)

used to predict the extreme wind speed of different return periods based on a large number of dependent samples. Then in order to verify the effectiveness of the ACER approach in estimating the extreme strains due to vehicle load and temperature, Monte Carlo (MC) simulations are conducted.

An in-service bridge is adopted to investigate the long-term effect of temperature as a real example. One year data of bridge strain are acquired from the structural health monitoring system installed on the Taiping Lake Bridge in China. The strain-time history is decomposed into two parts, i.e., the strain trend term and the fast varying part, using the analytical modal decomposition method (Wang and Chen 2013, Chen and Wang 2012). A linear regression model between the ambient temperature and the trend term of strain is set up. Then the EV distributions of strains due to vehicle load, temperature and the combination during the remaining service period are estimated by the ACER approach, respectively. Based on the estimation results, the temperature effect is analyzed. Finally, the reliability index and failure probability of the main girder of the bridge are calculated in two cases, with and without temperature effect.

2. Theoretical background

2.1 Analytical mode decomposition method

Wang (2013) proposed the analytical mode decomposition method for signals separation. For original time series $x(t)$ composed of n single components $x_i^{(d)}(t)$ (i=1, 2, …, n) with frequencies ω_1, ω_2, …, ω_n, ($\omega_i > 0$; i=1, 2,…, n), if the frequencies of each component ω_1, ω_2, …, ω_n ($\omega_i > 0$; i=1, 2,…, n), satisfy $\left(|\omega_1| < \omega_{b1}\right), \left(\omega_{b1} < |\omega_2| < \omega_{b2}\right), \cdots, \left(\omega_{b(n-2)} < |\omega_{n-1}| < \omega_{b(n-1)}\right)$ and $\left(\omega_{b(n-1)} < |\omega_n|\right)$, where $\omega_{bi} \in \left(\omega_i, \omega_{i+1}\right)$ (i=1, 2, …, n-1) denote n-1 bisecting frequencies, then every single component can be obtained analytically as follows

$$x_1^{(d)} = s_1(t), \cdots, x_i^{(d)}(t) = s_i(t) - s_{i-1}(t), \cdots, x_n^{(d)}(t) = x(t) - s_{n-1}(t) \quad (1)$$

$$s_i(t) = sin(\omega_{bi}t)\mathrm{H}\left[x(t)cos(\omega_{bi}t)\right] - cos(\omega_{bi}t)\mathrm{H}\left[x(t)sin(\omega_{bi}t)\right], \quad (i = 1, 2, \cdots, n-1) \quad (2)$$

where $\mathrm{H}\cdot[.]$ denotes Hilbert transform.

The strain-time history $x(t)$ of bridge is mainly due to the combination effect of ambient temperature and vehicle load, corresponding to low- and high-frequencies. Therefore, $x(t)$ can be decomposed into two single components by a appropriate cut-off frequency ω_b. Then the low frequency signal l(t) and the high frequency signal $h(t)$ can be obtained analytically as follows (Kuang *et al*. 2016)

$$\begin{aligned} h(t) &= sin(\omega_b t)\mathrm{H}\left[x(t)cos(\omega_b t)\right] - cos(\omega_b t)\mathrm{H}\left[x(t)sin(\omega_b t)\right] \\ l(t) &= x(t) - h(t) \end{aligned} \quad (3)$$

2.2 Conventional methods of extreme value estimation

EV theory indicates that EV estimation is only related to the tail of probabilistic distribution. Many techniques and models have been developed to describe these tails, by which the probabilities of EVs can be estimated on the basis of historical data. Among them, two of tail fitting approaches are extensively used which are the block maxima approach and the POT approach (Obrien *et al.* 2015). The block maxima approach divides the whole time history sample into equal size blocks and extracts maximum value for each block. These block maxima can be fitted to a Generalized Extreme Value (GEV) distribution (incorporating with Gumbel, Weibull and Fréchet distribution) (Xia and Ni 2016). The block of time (an hour, a day, a year, etc.) should be determined carefully to ensure that these block maxima are independent. A significant drawback of this approach is that the data information is wasted. Several independent data may be collected in one block but only the largest data point is used, even if the values of some data points in the block are larger than the maximum value of other blocks. In such a case, the POT approach can retain all those tail data. The POT approach extracts all independent peaks over a selected threshold. The distribution of these peaks is approximating a General Pareto Distribution (GPD) (Gu *et al.* 2014). The POT approach avoids the data information's low utilization problem of the block maximum approach, while selecting an appropriate threshold is critical and challenging.

The two conventional approaches have a prerequisite that data for EV estimation is required to be independent. However, in civil engineering, the collected data usually shows significant correlation between the adjacent data points. As shown in Fig. 1, taking the strain data obtained from a sensor installed on girder when a vehicle passes through the bridge as an example (the sampling frequency is 50 Hz), it can be found that many data points beyond the level of x, but only the strain peak should be selected for the EV estimation since the exceedances are not independent. In this case, the independent data are easy to be extracted. However, for complex time series such as the strain data due to temperature whose underlying variation period is unknown, the conventional methods are not suitable for its EV estimation any more. The reason is that choosing independent data points objectively will result in errors easily.

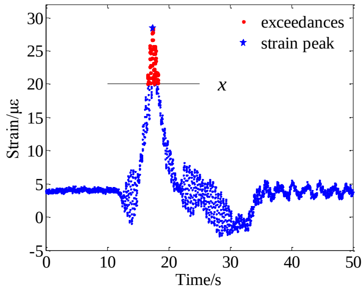

Fig. 1 The strain time-history due to a vehicle

2.3 Average conditional exceedance rate approach

Based on the conditional probability and Markov process, Naess and Gaidai (2009) proposed the ACER approach for EV estimation. This approach has similar aspects to the POT approach but it deals with exceedance rate instead of peaks. A significant advantage of the ACER approach is that it can eliminate the effect of data dependence on EV estimation through conditional exceedance rate. The issue of declustering of data to ensure independence can be avoided, which is a common problem for the two conventional methods. Therefore, the ACER approach is more appropriate to deal with the strain data due to temperature effect of which the underlying variation period is difficult to be determined.

Let $\{X_1, X_2, \ldots, X_N\}$ denote the observation samples of the stochastic process $X(t)$ collected at the discrete times $\{t_1, t_2, \ldots, t_N\}$ in $(0, T_m)$. Assuming that each random variable $\{X_j | k \leq j \leq N\}$ is depend on previous k-1($2 \leq k \leq j$) random variables, the cumulative probability function (CDF) of the EV of $X(t)$ during the prediction period T_p, which is supposed to be much longer than the measurement period T_m, can be obtained as follows(Ding and Chen 2014)

$$F_M(x) = \exp\left(-\nu T_p \alpha(x)\right) \tag{4}$$

where $\alpha(x)$ denotes the conditional exceedance rate, i.e., the exceedance probability conditional on k-1 previous non-exceedances, $\alpha(x) = \alpha_{kj}(x) = P\{X_j > x \,|\, X_{j-1} \leq x, \ldots X_{j-k+1} \leq x\}$. The v parameter denotes the occurrence frequency of continuous k-1 non-exceedances. The empirical estimation of v can be obtained by $v=N_B/T_m$, where N_B denotes the number of occurrences of continuous k-1 non-exceedances during measurement period T_m. The conditional exceedance rate $\alpha(x)$ can be estimated by introducing ACER $\bar{\alpha}(x)$ (Naess and Gaidai 2009)

$$\alpha(x) \approx \bar{\alpha}(x) = \frac{1}{N-k+1}\sum_{j=k}^{N} \alpha_{kj}(x) \approx \lim_{N\to\infty} \frac{\sum_{j=k}^{N} I(A_{kj})}{N-k+1}, \qquad j = k, \ldots, N, k = 2, 3, \ldots \tag{5}$$

in which A_{kj} represents the event that the j^{th} random variable X_j exceeds the level of x while previous continuous k-1 random variable don't. $I(A_{kj})$ denotes the function of event A_{kj}. It is equal to 1 if the event occurs, otherwise it is equal to 0.

Assuming that the appropriate asymptotic EV distribution for the observation samples under study is Gumble distribution, the upper tail of $\alpha(x)$ can be described as follows

$$\alpha(x) = q\exp\left(-\frac{(x-\mu)^{\xi}}{\sigma}\right), \quad x > u, \sigma > 0 \tag{6}$$

where q, μ, σ and ξ are suitable constants, and u is a large threshold. The parameters (q, μ, σ and ξ) can be optimized

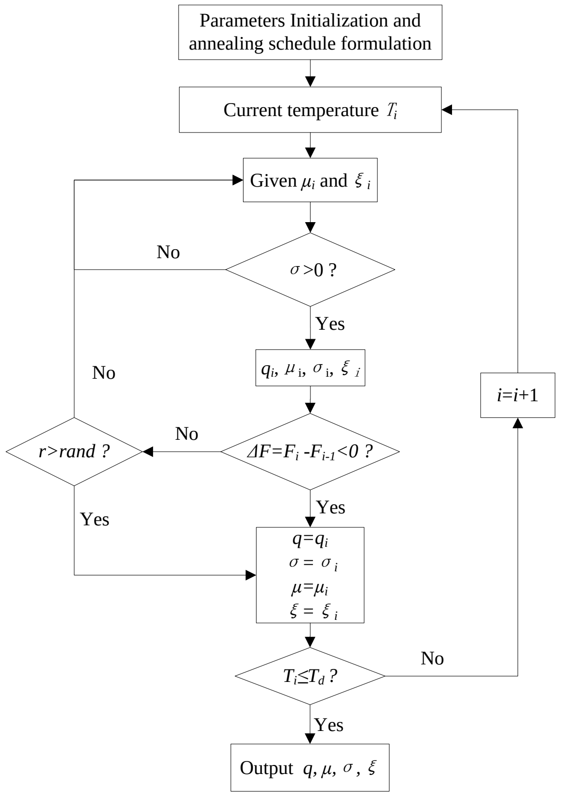

Fig. 2 Flowchart of parameters estimation of q, μ, σ and ξ

by the fast simulated annealing algorithm (Inger 1989) and the least squares method. The steps are as follows

(I) An annealing schedule is formulated as $T_i = T_0 \exp[-\alpha_1 (i-1)^{1/2}]$, in which T_i, T_0, α_1, i denote the current temperature, initial temperature, attenuation coefficient and iteration number respectively. The final temperature T_d and the initial values of μ and ξ are determined.

(II) According to value ranges of μ and ξ, i.e., $\min(X_j \,|\, j=1, \ldots, N) < \mu \leqslant u$, $0 < \xi < 5$, the perturbation models are given as $\mu_i = \min(X_j) + rand \cdot [u - \min(X_j)]$, $\xi_i = 5 \cdot rand$, $rand \in (0, 1)$.

(III) Let $y_l = \log\alpha(x_l)$, $t_l = (x_l - \mu)^{\xi}$, where x_l $(1 \leqslant l \leqslant m)$ denotes the upcrossing level. Substituting y_l and t_l into Eq. (6), the estimators σ and q can be obtained by the least squares method as $\sigma_i = -\sum_{l=1}^{m} w_l (t_l - \bar{t})^2 / \sum_{l=1}^{m} w_l (t_l - \bar{t})(y_l - \bar{y})$, $q_i = \exp(\bar{y} + \bar{t}/\sigma_i)$ with $\bar{y} = \sum_{l=1}^{m} w_l y_l$ and $\bar{t} = \sum_{l=1}^{m} w_l t_l$, in which $w_l = [\log CI^{+}(x_l) - \log CI^{-}(x_l)]^{-2} / \sum_{l=1}^{m} [\log CI^{+}(x_l) - \log CI^{-}(x_l)]^{-2}$ represents weight factors putting more emphasis on the more reliable estimates. $CI^{+}(x_l)$ and $CI^{-}(x_l)$ denote the upper bound and lower bound of the 95% confidence interval of $\alpha(x_l)$.

(IV) According to the value range of σ (i.e., σ>0), check the estimated value of σ_i. If $\sigma_i \leqslant 0$, return back to step (II), that is, μ_i and ξ_i need to be re-determined.

The objective optimization function $F(q, \mu, \sigma, \xi)$ can be established by the squared residuals minimum standard as

$$F_i(q,\mu,\sigma,\xi)=\sum_{l=1}^{m} w_l \left|\log\alpha(x_l)-\log q+(x_l-\mu)^{\xi}/\sigma\right|^2 .$$

Difference between the old objective function and the new one is calculated (i.e., $\Delta F=F_i - F_{i-1}$). An acceptance criteria model of the parameters (q, μ, σ, ξ) is established according to Metropolis criterion as follows

i. $\Delta F < 0$, the new model will be accepted.

ii. $\Delta F \geqslant 0$, set $r = \min(\exp(-\Delta F/a_0T_i), 1)$, and generate random number $rand \in (0, 1)$, where $a_0>0$ is a constant. Then if $r > rand$, the new model will be accepted, otherwise rejected.

As shown in Fig. 2, iterative calculations should be implemented until $T_i \leqslant T_d$. Then the optimized parameters can be obtained. In addition, repeated trials show that different thresholds have little effect on the EV estimation when the threshold u is large enough (i.e., $\alpha(u)<0.05$).

3. Theoretical examples

To validate the feasibility of the ACER approach in predicting EV of bridge strain due to load effect or temperature effect, MC simulations are conducted.

3.1 Exteme strain prediction due to vehicle load based on Monte Carlo simulation

The maximum strain of the measuring point induced by a vehicle passing through a bridge is defined as strain peak. According to the EV theory (Shi 2006), the EV estimation of vehicle load effect depends on large strain peaks. To ascertain the probability distribution of those data, several mixed distributions are chosen to fit the strains peaks over a moderate threshold (1.8×10^{-5}) of a real bridge. Results show that a mixed distribution of one Weibull and two Normal distributions can described these data well as follows

$$f(x)=\frac{p_1\xi_w}{\sigma_w}\left(\frac{x-\mu_w}{\sigma_w}\right)^{\xi_w-1}\exp\{-(\frac{x-\mu_w}{\sigma_w})^{\xi_w}\}+\frac{p_2}{\sigma_{N1}\sqrt{2\pi}}\exp\{-\frac{(x-\mu_{N1})^2}{2\sigma_{N1}^2}\}+\frac{p_3}{\sigma_{N2}\sqrt{2\pi}}\exp\{-\frac{(x-\mu_{N2})^2}{2\sigma_{N2}^2}\} \quad (7)$$

in which p_1, p_2 and p_3 are weighting coefficients satisfying $p_1+ p_2 +p_3=1$.σ_W, ξ_W , μ_W represent the scale parameter, shape parameter and location parameter of Weibull distribution, and μ_{N1}, μ_{N2}, σ_{N1}, σ_{N2} parameters denote the mean values and standard deviations of Normal distributions. To simulate the tail distribution of vehicle load effect, Eq. (7) is assumed as the parent distribution of tail data of strain peaks. Parameters of the mixed distribution are listed in Table 1.

The MC simulation is used to generate a 1000-day period of sampled data from the parent distribution, and 500 strain peaks are produced in each day, i.e., 500000 data points in total. These sampled data is independent and identically distributed. Both the ACER approach and the conventional approaches are employed to estimate the EV distributions of yearly, 10-yearly, 20-yearly and 100-yearly.

Table 1 Parameters of the parent distribution

Component	Weibull distribution	Normal distribution	Normal distribution
Weighting coefficient	0.65	0.2	0.15
Parameter	σ_W=5, ξ_W=1.0, μ_W=18	μ_N=21, σ_N=0.8	μ_N=23, σ_N=2

The average conditional exceedance rates versus upcrossing levels taking k=1, k=2, k=4 and k=8 are shown in Fig. 3(a). All average conditional exceedance rate functions (ACERFs) converge to the ACERF of k=1 when the upcrossing level is higher than 3×10^{-5}. It verifies that the sampled data is independent. It can also be found that when the upcrossing level is low (x<30) and k is large (k=4, 8), data below the threshold is limited in number, for which large error is easily brought in the calculation of ACER. Therefore, the threshold of the ACER approach should be large enough. The right tail of the ACERF of k=1 is fitted to Eq. (6). Its optimal fitting and 95% confidence interval are shown in Fig. 3(b). Substituting the fitting results and different prediction periods (1, 10, 20 and 100 years) into Eq. (4), the extreme strain distributions and its expectations can be obtained as shown in Fig. 4(a).

The EV distributions are also estimated by the conventional approaches. Daily maxima, i.e., 1000 data points, are extracted to be fitted by a GEV distribution. Its parameters are estimated by the maximum likelihood estimation. The fitting shape parameter is close to zero and negative. Obviously it is not reasonable. So let the shape parameter be zero, that is, the parent distribution is in the Extreme Type I domain of attraction. The EV distributions of different prediction periods can be obtained by raising the fitting Gumble distribution to corresponding powers, as shown in Fig. 4(b). The expectations of these EV distributions are also shown in the figure. The POT approach is another method used to predict the EVs. Strain peaks over a high threshold (5×10^{-5}) are selected to be fitted by a GPD. The fitting shape parameter of the GPD is similar with that of the GEV distribution, which is close to zero and negative. Likewise, let the shape parameter be zero. The EV distributions and its expectations are obtained by raising the GPD to different powers as shown in Fig. 4(c).

Raising the parent distribution to the 180000th, 1800000th, 3600000th and 18000000th power respectively, the theoretical distributions of EV and expectations can be obtained, as shown in Fig. 4(d).

From Fig. 4, it can be found that the estimates by ACER approach are similar with that by POT approach. The reason is that the data used in both approaches is almost the same, only with little difference in the threshold. The estimates by the two approaches are smaller than the theoretical results, while the estimates by the block maxima approach are larger than the theoretical results generally. Overall, The EVs estimated by the ACER approach are closer to the theoretical value than that by conventional approaches, which means that the ACER approach is more accurate than those conventional methods.

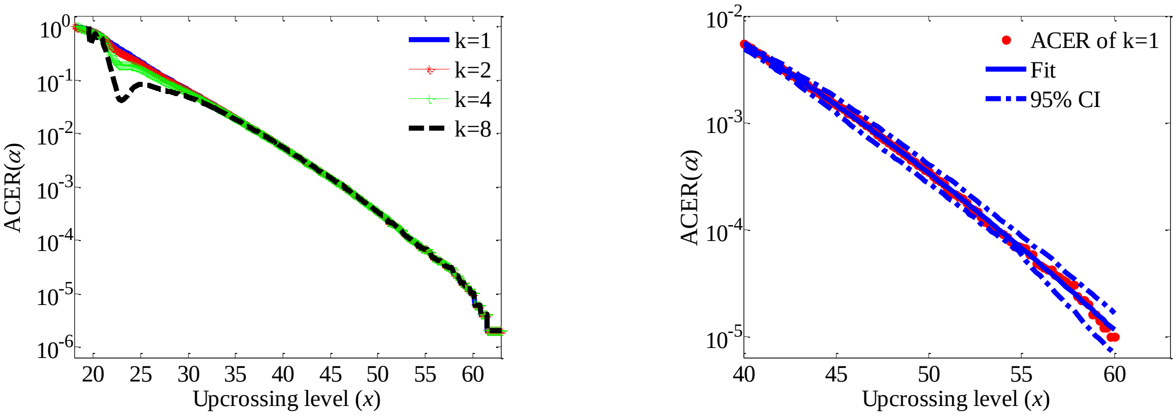

(a) the ACERFs of different k values (b) The optimized fit for ACERF of k=1

Fig. 3 ACER of the strain due to vehicle load (MC simulation)

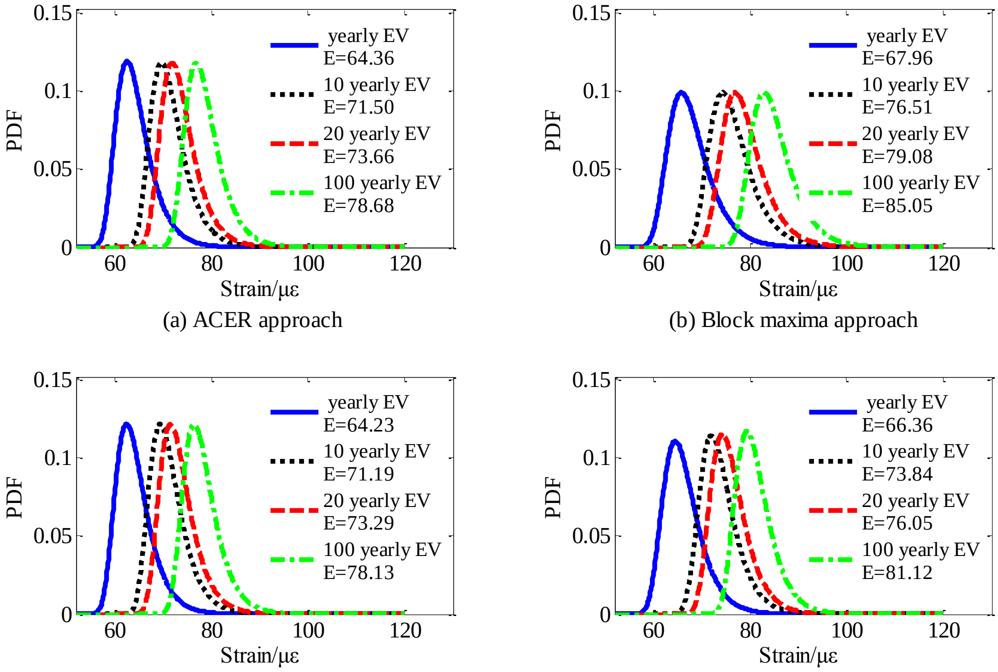

(a) ACER approach (b) Block maxima approach

(c) POT approach (d) Theoretical value

Fig. 4 Estimated EV distributions and theoretical value (MC simulation)

3.2 Extreme strain prediction due to temperature effect based on Monte Carlo simulation

Hourly maxima of strain due to temperature at the same hour every day are supposed to be independent and normally distributed. A 24-dimensional Gaussian distribution, the mean and covariance matrix of which are obtained by the measured strain data of a real bridge, is used as the parent distribution of strain due to temperature. Then 1000 days of strain data, i.e., 24000 data points are sampled by the MC simulation. These data is obviously dependent. Therefore, conventional methods cannot be used to estimate the EV, and only the ACER approach is used.

The conditional exceedance rates versus upcrossing levels taking different k values are shown in Fig. 5(a). The ACERFs of k=4 and k=8 converge to the ACERF of k=2, which are different from that of k=1. It reveals that there is significant correlation among the sampled data and the effect is removed for the ACERF of k=2, then it can be used to estimate the EV. Fig. 5(b) shows the optimal fitting for $\alpha(x)$ of k=2 and its 95% confidence interval. The estimated EVs and the expectations are shown in Fig. 6(a), while corresponding theoretical results are shown in Fig. 6(b). These two figures show that the EVs estimated by the ACER approach are well consistent with the theoretical results, which verifies the effectiveness of the ACER approach in predicting the extreme strain induced by temperature effect.

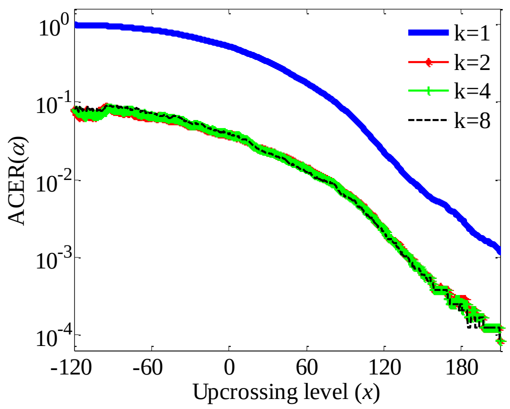

(a) the ACERFs of different k values

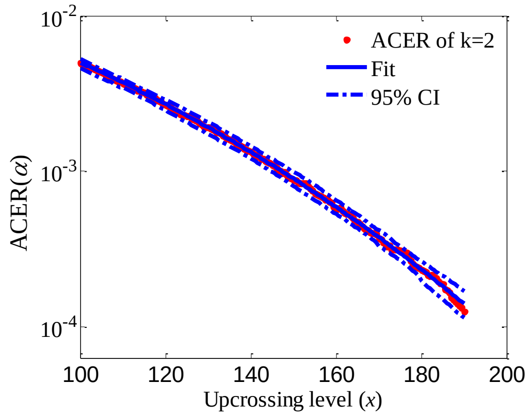

(b) The optimized fit for ACERF of k=2

Fig. 5 ACER of the strain due to temperature (MC simulation)

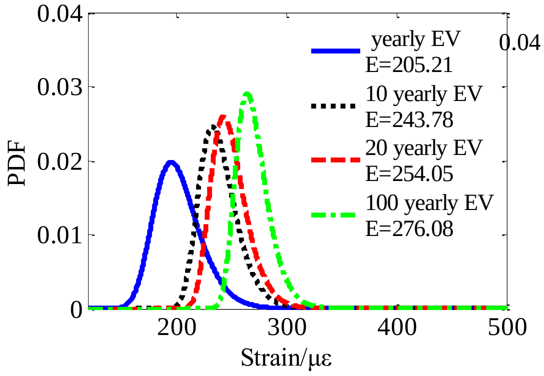

(a) ACER method

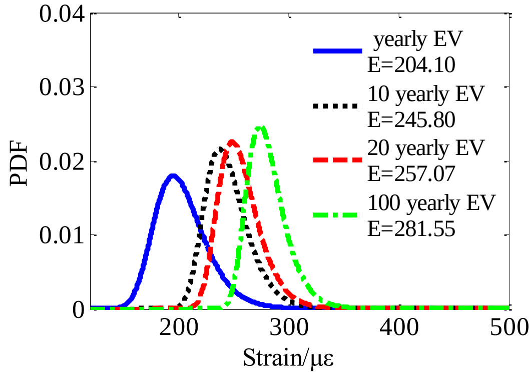

(b) Theoretical value

Fig. 6 Estimated EV distributions and theoretical value (MC simulation)

4. Temperature effect analysis on strain of the Taiping Lake Bridge

The Taiping Lake Bridge is a pre-stressed concrete cable-stayed bridge with single-tower and single cable plane, located on the G205 nation highway over the Taiping Lake in Huangshan scenic spot, Anhui Province, China (Yan and Ren 2016). The bridge has a length of 380 m (span combination: 190m+190m), as shown in Fig. 7. The bridge carries four lanes with a width of 14 m. The main girder has a 3-cell single box pre-stressed concrete box-girder with inclined webs. The tower is of reinforced concrete. The bridge has a total of 27×2=54 stay cables, showing sector symmetric arrangement.

The health monitoring system was installed on the bridge in 2014 to obtain the service status in real time. Based on the finite element model of the bridge, measurement points were selected to be located in the middle of two adjacent cables. Strain gauges were installed at the upper surface of bottom plate of the box girder. The diagram of the elevation and the cross section installed with strain gauges are shown in Figs. 8(a) and 8(b). The scene of strain gauge and temperature compensation piece are shown in Fig. 9(a). Fig. 9(b) shows the hardware and software of NI data acquisition card. The sampling frequency of dynamic strain is 50 Hz, and the sampling frequency of temperature is 0.083 Hz.

Fig. 7 The Taiping Lake Bridge

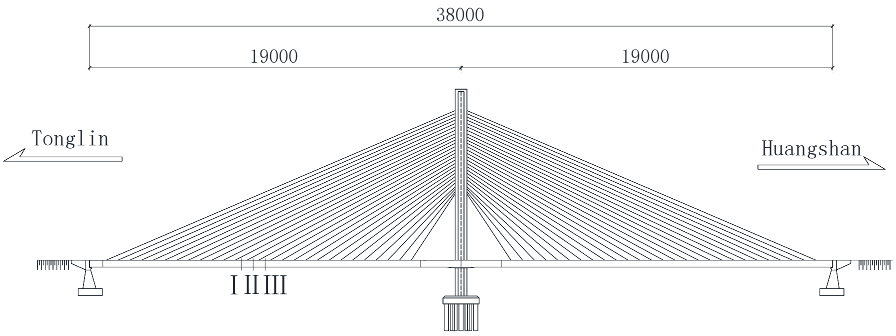

(a) Elevation

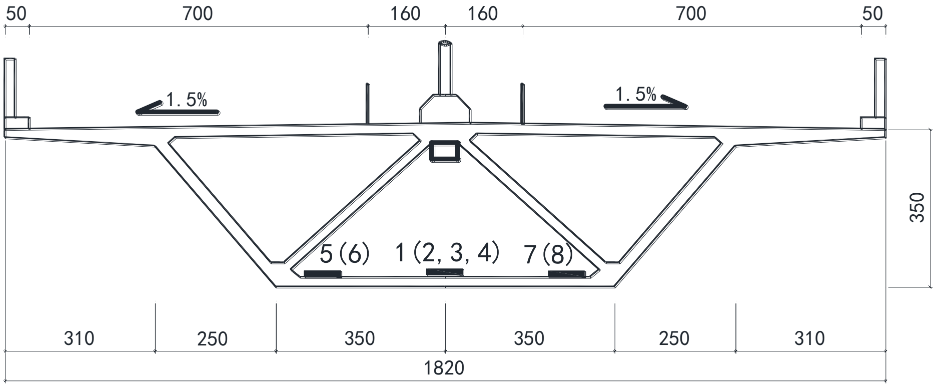

(b) Cross section

Fig. 8 Arrangement of measuring points

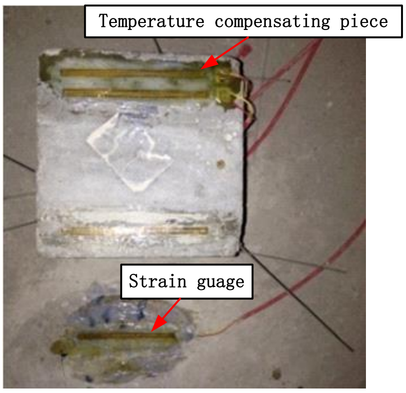

(a) Strain gauge

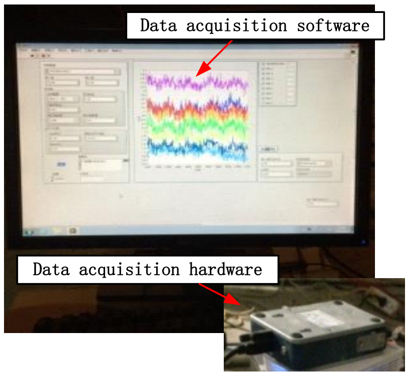

(b) Data acquisition system

Fig. 9 Monitoring site of the Taiping Lake Bridge

4.1 Correlation characteristics between environmental temperature and strain

4.1.1 Decomposition of measured strain-time history

The measured ambient temperature and strain on 27th December, 2015 are shown in Figs. 10(a) and 10(b). Fig. 10(b) reflects that the measured dynamic strain is mainly composed of two parts, i.e., the trend term of strain and the "jump". It can be found that the strain trend term is significant correlated with the temperature. A magnified "jump", as shown in the upper-left of Fig. 10(b), is obviously due to a vehicle passing through the bridge.

Previous studies indicate that the measured strain-time history is mainly induced by temperature variation and vehicle load (Wu *et al.* 2014). Same conclusion can be drawn from in this paper.

The time of a vehicle passing through the bridge is about 30 seconds, while temperature variation period is approximately 24 hours, or even longer. Since the frequencies differ greatly, the measured strain-time history can be decomposed into two single components by the analytical mode decomposition method, as shown in Fig. 11. The trend term of measured strain due to temperature is shown in Fig. 11(a), and the fast varying part due to vehicle load is shown in Fig. 11(b).

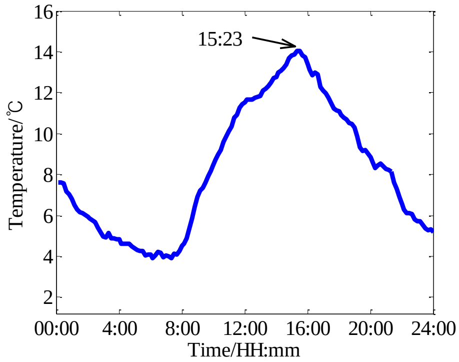

(a) Ambient temperature

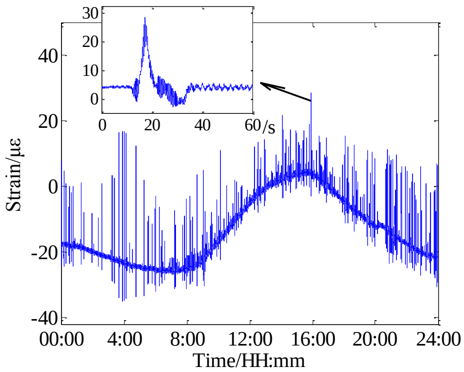

(b) Strain-time history

Fig. 10 Measured data of the Taiping Lake Bridge on 27th December 2015

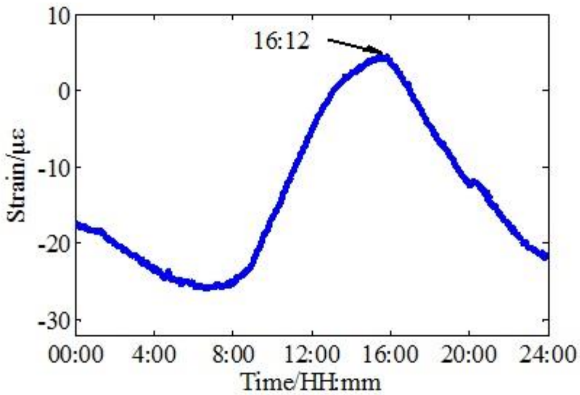

(a) The trend term of strain

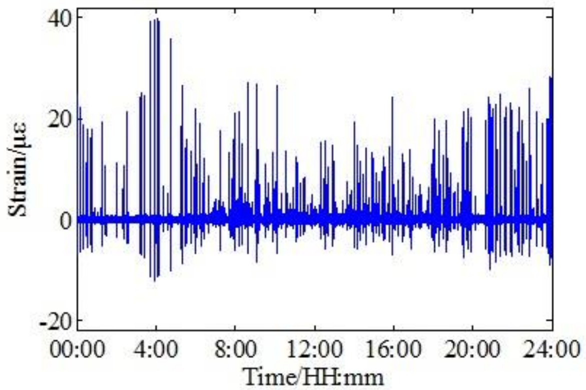

(b) The fast varying part

Fig. 11 The decomposition of measured strain-time history of 27th December 2015

4.1.2 Correlation analysis of the trend term of measured strain and ambient temperature

As shown in Figs. 10(a) and 11(a), the highest temperature of the day (27th December 2015) occurred at 15:23, while the maximum value of the strain trend term occurred at 16:12. Apparently, the variation of strain lags behind the temperature for about one hour. Same conclusion can be drawn from the available data of 355 days (from August 2015 to July 2016).

The temperature is positively correlated with strain trend term as shown in Figs. 10(a) and 11(a), with a correlation coefficient of 0.983. The correlation between the strain trend term and the ambient temperature is also studied using the data of 355 days. The scatter plot for the daily mean temperature and daily mean trend term of strain is shown in Fig. 12, of which the correlation coefficient is 0.86. A linear regression line and 95% confidence interval are also shown in the figure, with gradient 4.3 and intercept -38.46. It means that for every 1℃ increase in temperature, the stress of measuring point increase by 0.148MPa.

4.2 The extreme strain distribution prediction of strain

Based on the measured strain data of 355 days, the strain induced by vehicle load and temperature are separated by the analytical mode decomposition method. Then the EV distributions of the two parts and the measured strain data during the remaining service period are predicted by the ACER approach, respectively.

4.2.1 The extreme strain prediction due to vehicle load

As shown in Fig. 13, the maximum value of each "jump" is the strain peak. Since small values are irrelevant to the EV distribution, only those strain peaks larger than 5 $\times 10^{-6}$ are extracted. The comparison chart of the ACERFs taking different k values is shown in Fig. 14(a). A rather strong statistical independence between the extracted data has been reflected in this figure, since all ACERFs converge in the far tail.

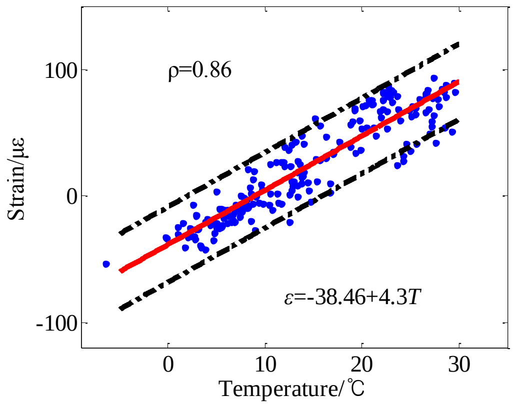

Fig. 12 Scatter diagram of daily mean temperature and daily mean trend term of strain

That is, the strain peaks due to vehicle load are independent (Gong *et al*. 2014). Therefore, the ACERF of k=1 is used to estimate the EV. Fig. 14(b) shows its optimal fitting and 95% confidence interval. Substituting the fitting results into Eq. (4), the EV distribution of strain due to vehicle load during the remaining service period of the bridge can be obtained as shown in Fig. 15.

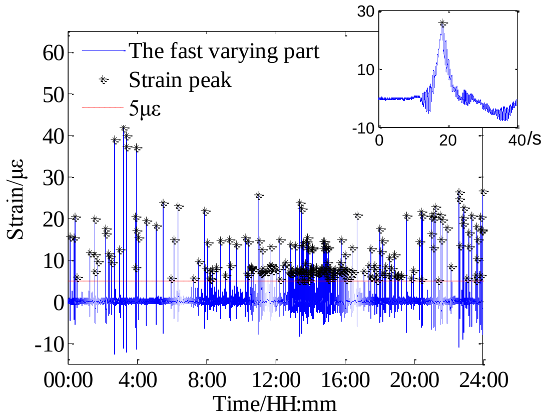

Fig. 13 Strain peaks due to vehicle loads of 27th December 2015

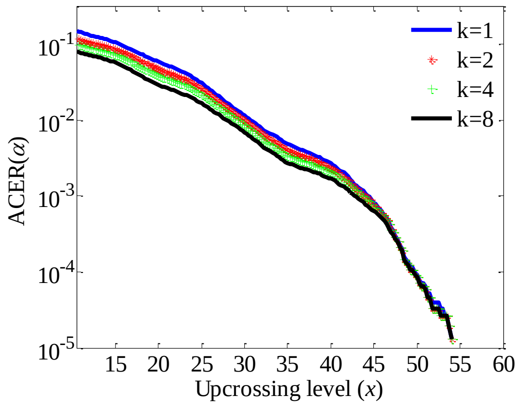

(a) the ACERFs of different k values

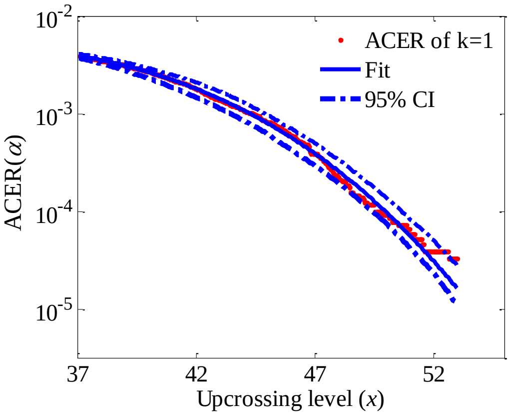

(b) The optimized fit for ACERF of k=1

Fig. 14 ACER of the strain due to vehicle load

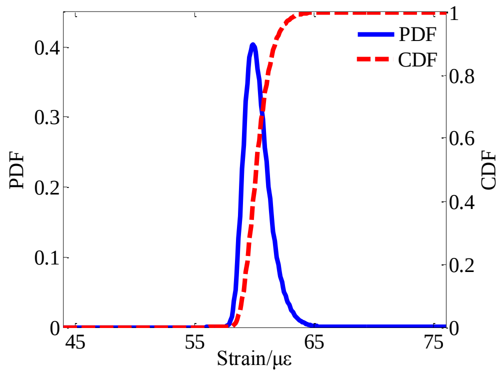

Fig. 15 Predicted EV distribution of strain due to vehicle load

4.2.2 The extreme strain prediction due to temperature effect

The hourly maxima of strain trend term shown in Fig. 11(a) are extracted to estimate the extreme strain due to temperature effect. Since the trend term of strain is closely related to temperature time series, there should be correlation among those extracted data. The comparison chart of the ACERFs taking different k values is shown in Fig. 16(a). Like the Fig. 5(a), an obvious correlation can be found between the consecutive data, which are clearly reflected in effect of conditioning on the previous data. Therefore, ACERF of k=2 is adopted to estimate the EV. The optimal fitting for $\alpha(x)$ taking k=2 and its 95% confidence interval are shown in Fig. 16(b). Substituting the fitting results into Eq. (4), the EV distribution of strain due to temperature variation during the remaining service period of the bridge can be obtained and shown in Fig. 17.

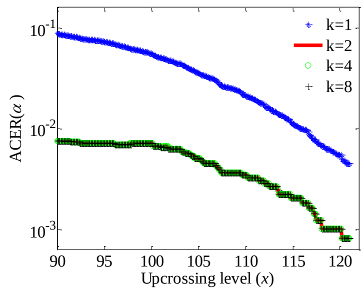

(a) the ACERFs of different k values

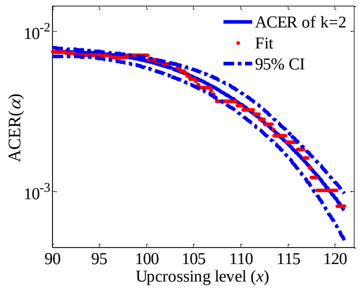

(b) The optimized fit for ACERF of k=2

Fig. 16 ACER of the strain due to temperature

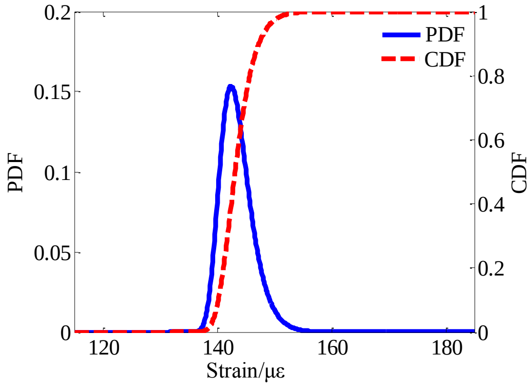

Fig. 17 Predicted EV distribution of strain due to temperature variation

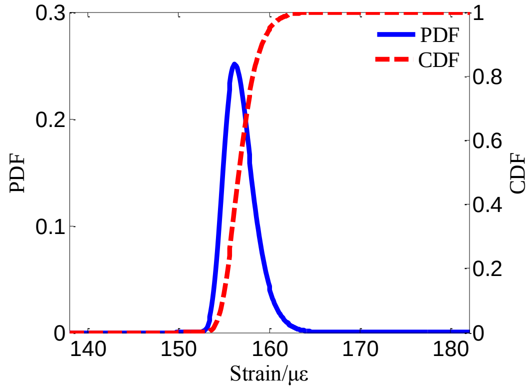

Fig. 19 Predicted EV distribution of strain due to the combination effect

4.2.3 The extreme strain prediction due to combination effect of temperature and vehicle load

The hourly maxima of the original strain are selected to estimate the extreme strain due to the combination effect. These sampled data also should be dependent since the temperature effect is included. The comparison chart of the ACERFs taking different k values is plotted in Fig. 18(a). Being similar with Figs. 16(a) and 5(a), ACERF of k=2 is adopted to estimate the EV distribution. Its optimal fitting and 95% confidence interval are shown in Fig. 16(b). According to Eq. (4), the EV distribution of strain due to the combination effect during the remaining service period of the bridge are obtained as shown in Fig. 19.

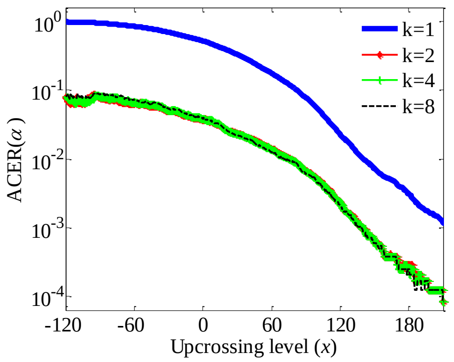

(a) the ACERFs of different k values

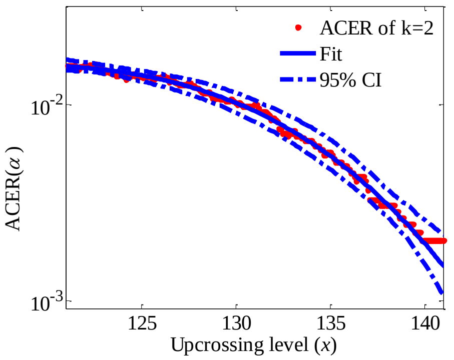

(b) The optimized fit for ACERF of k=2

Fig. 18 ACER of the strain due to combination effect

4.3 Prediction results analysis of extreme strain

The prediction results of the extreme strain due to vehicle load, temperature, and the combination effect are listed in Table 2. It shows that the EV due to the combination effect of temperature and vehicle load is larger than that due to either of them alone, and smaller than the summation. This observation can be illustrated by the fact that the daily maximum strain induced by temperature and vehicle load appears at different times. As shown in Fig. 11, the maximum strain due to temperature appears at about 16:00, while that due to vehicle load appears at about 04:00. The table also reveals that the 95% quantile of extreme strain distribution due to temperature is 2.38 times larger than that due to vehicle load. Located on national highway, the Taiping Lake Bridge has small traffic volume. There are rarely two or more heavy vehicles on the bridge at the same time, so the extreme strain due to vehicle load is relatively small.

4.4 Reliability estimation based on extreme strain distributions

Reliability index has played fundamental roles in structural health monitoring and risk analysis, which can be calculated using various efficient simulation approaches (Wang *et al.* 2016). In this study, reliability indexes and failure probabilities of the main girder of Taiping Lake Bridge are obtained using Monte Carlo Simulation approaches, whose results are listed in Table 3.

By assuming that the measuring point was designed to bear 7×10^{-5} (i.e., 2.42MPa) due to live loads (i.e., vehicle load and temperature), the failure probability is 8×10^{-7} and reliability index is 8.3 if vehicle load is taken into account only, but the failure probability rises to 1 and the reliability index falls to below zero when the temperature effect is included. Similarly, if the ultimate stress due to live loads of the measuring point is designed to be 1.7×10^{-4} (i.e., 5.87MPa), the failure probability rises from almost zero to 2×10^{-7} and the reliability index falls from 72 to 7.5 when the temperature effect is considered.

Table 2 Prediction results of the EV distribution of strain

Load type		Vehicle load	Ambient temperature	Combination effect
Expectation of the EV distribution	Strain ($\times 10^{-6}$)	60.5	143.6	156.8
	Stress/MPa	2.09	4.95	5.41
95% quantile of the EV distribution	Strain ($\times 10^{-6}$)	62.5	148.8	160.1
	Stress/MPa	2.16	5.13	5.52

Table 3 Reliability estimation of the main girder of Taiping Lake Bridge

Ultimate strain ($\times 10^{-6}$)	Ultimate stress /MPa	Vehicle load alone		Temperature effect being included	
		Reliability index	Failure Probability	Reliability index	Failure Probability
70	2.42	8.3	8×10^{-7}	< 0	1
170	5.87	72	--*	7.5	2×10^{-7}

*--: The failure probability is too small to calculate, and is much lower than (1×10^{-16}).

The table reflects that reliability index drops rapidly when temperature effect is considered. It can also be found that under the condition that the failure probability and reliability index are almost identical, the carrying capacity of measuring point should be increased from 7×10^{-5} to 1.7×10^{-4} when temperature effect is included.

5. Conclusions

This study developed the EV of bridge strain to investigate the long-term effect of temperature. The ACER approach is verified and adopted to estimate the extreme strain. Based on 355 days data of strain and temperature acquired from a long span cable-stayed bridge in Anhui Province of China, the strains due to vehicle load and temperature are obtained by decomposing the measured strain-time history into two parts. The linear regression equation and the correlation coefficient of environmental temperature and strain trend term are determined. The extreme strain distributions due to vehicle load, temperature and the combination during the remaining service period are estimated. Finally, the estimation results are applied in reliability analysis. According to the numerical simulation and example application, the conclusions can be drawn as follows:

- The MC simulations reveal that the extreme strain due to vehicle load estimated by the ACER approach is much closer to the theoretical results than the conventional approaches. The ACER approach can eliminate the effect caused by relativity between sampled data, and the extreme strain due to temperature effect can be obtained.
- Linear correlation can be found between the temperature and trend term of strain with a correlation coefficient of 0.86. The regression equation shows that for every 1°C increase in temperature, the stress is increased by 0.148 MPa. Moreover, the variation of strain lags behind the ambient temperature for about one hour.
- The EV estimation results show that the 95% quantile of extreme strain distribution induced by temperature is up to 1.488×10^{-4} (5.13 MPa) which is 2.38 times larger than that induced by vehicle load.
- Taking into account of the temperature effect, the carrying capacity of the measuring point should be increased from 7×10^{-5} to 1.7×10^{-4} with nearly the same failure probability and reliability index.

References

Branco, F.A. and Mendes, P.A. (1993), "Thermal actions for concrete bridge design", *J. Struct. Eng.- ASCE*, **119**(8), 2313-2331.

Catbas, F.N., Susoy, M. and Dan, M.F. (2008), "Structural health monitoring and reliability estimation: long span truss bridge application with environmental monitoring data", *Eng. Struct.*, **30**(9), 2347-2359.

Chen, G.D. and Wang, Z.C. (2012), "A signal decomposition theorem with Hilbert transform and its application to narrowband time series with closely spaced frequency components", *Mech. Syst. Signal Pr.*, **28**(2), 258-279.

Ding, J. and Chen, X.Z. (2014), "Assessment of methods for extreme value analysis of non-Gaussian wind effects with short-term time history samples", *Eng. Struct.*, **80**, 75-88.

Duan, Y.F., Li, Y. and Xiang, Y.Q. (2010), "Correlation analysis of structural stress responses and temperature of a tied arch bridge using long-term health monitoring data", *Proceedings of the 6th International Conference on Arch Bridges*, Fuzhou, China, October.

Gindy, M. and Nassif, H.H. (2006), "Comparison of traffic load models based on simulation and measured data", *Proceedings of the Joint International Conference on Computing and Decision Making in Civil and Building Engineering*, Montreal, Canada, June.

Gong, K.M., Ding, J. and Chen, X.Z. (2014), "Estimation of long-term extreme response of operational and parked wind turbines: Validation and some new insights", *Eng. Struct.*, **81**, 135-147.

Gu, Y.M., Li, S.L., Li, H. and Guo, Z.M. (2014), "A novel Bayesian extreme value distribution model of vehicle loads incorporating de-correlated tail fitting: Theory and application to the Nanjing 3rd Yangtze River Bridge", *Eng. Struct.*, **59**(2), 386-392.

Han, H.T. (2006), "Analysis and investigation the upgrading and modifying project of Jiangyin Bridge structural health monitoring (SHM) system", M.S. Dissertation; Hohai University, Nanjing, China.

Inger, L. (1989), "Very fast simulated reannealing", *Math. Conut. Model.*, **12**(8), 967-973.

James, G. (2003), "Analysis of traffic load effects on railway bridges", Ph.D. Dissertation; Royal Institute of Technology, Sweden, Stockholm.

Karpa, O. and Naess, A. (2013), "Extreme value statistics of wind speed data by the ACER method", *J. Wind Eng. Ind. Aerod.*, **112**(1), 1-10.

Krkoška, L. and Moravčík, M. (2015), "The analysis of thermal effect on concrete box girder bridge", *Procedia Eng.*, **111**, 470-477.

Kuang, K.S.C., Li, D. and Koh, C.G. (2016), "Acoustic emission source location and noise cancellation for crack detection in rail head", *Smart Struct. Syst.*, **18**(5), 1063-1085.

Li, M., Ren, W.X., Yang, X., Liu, J.L. and Wang, N.B. (2014),

" AMD-based Novelty Detection of Structure Using Dynamic Strains", *Proceedings of the 13th International Symposium on Structural Engineering*, Hefei, China, October.

Li, Z.X., Wu, B.J. and Wang, Y. (2009), "Statistical analyses on multi-scale features of monitoring data from health monitoring system in long cable supported bridges", *Procedia Eng.*, **1**, 123-127.

Naess, A. and Gaidai, O. (2009), "Estimation of extreme values from sampled time series", *Struct. Saf.*, **31**(4), 325-334.

Obrien, E.J., Enright, B. and Getachew, A. (2010), "Importance of the tail in truck weight modeling for bridge assessment", *J. Bridge Eng.*, **15**(2), 210-213.

Obrien, E.J., Schmidt, F., Hajializadeh, D., Zhou, X.Y., Enright, B., Caprani, C.C., Wilson, S. and Sheil, E. (2015), "A review of probabilistic methods of assessment of load effects", *Struct. Saf.*, **53**, 44-56.

Saetta, A., Scotta, R. and Vitaliani, R. (1995), "Stress analysis of concrete structure subjected to variable thermal loads", *J. Struct. Eng. - ASCE*, **121**(3), 446-457.

Shi, D.J. (2006), *Practical extremum statistical method*, Science and Technology Press, Tianjin, China.

Wang, Z.C. and Chen, G.D. (2013), "Analytical mode decomposition of a time series with overlapping and rapidly time-varying frequencies with Hilbert transform", *Smart Mater. Struct.*, **22**(9), 1-15

Wang, J., Katafygiotis. L.S. and Feng, Z.Q. (2016), "An efficient simulation method for the first excursion problem of linear structures subjected to stochastic wind loads", *Comput. Struct.*, **166**(1), 75-84.

Wong, K.Y. (2004), "Instrumentation and health monitoring of cable-supported bridges", *Struct. Control Health Monit.*, **11**(2), 91-124.

Wu, B.J., LI, Z.X., Chan, Tommy H.T. and Wang, Y. (2014), "Multiscale features and information extraction of online strain for long-span bridges", *Smart Struct. Syst.*, **14**(4), 679-697

Xia, Y.X. and Ni, Y.Q. (2016), "Extrapolation of extreme traffic on bridges based on long-term SHM data", *Smart Struct. Syst.*, **17**(6), 995-1015.

Yan, W.J. and Ren, W.X. (2016), "Circlularly-symmetric complex normal ratio distribution for scalar transmissibility functions, Part II: Probabilistic model and validation", *Mech. Syst. Signal Pr.*, **80**(1),78-98.

BS